MULTI-OBJECTIVE OPTIMIZATION OF MAGNETORHEOLOGICAL CLUTCH WITH STATIONARY HOUSING

Bui Quoc Duy[1] , **Le Duc Thang**[2], **Diep Bao Tri**[1],
Nguyen Ngoc Diep[1], **Nguyen Quoc Hung**[2,*]

[1]*Faculty of Mechanical Engineering, Industrial University of Ho Chi Minh City, Vietnam*
[2]*Faculty of Engineering, Vietnamese-German University (VGU), Vietnam*
*E-mail: hung.nq@vgu.edu.vn

Abstract. This study focuses on the development of magnetorheological fluid (MRF) based clutch systems for speed control of a rotary load. A new configuration for speed control of a rotary shaft using a magnetorheological clutch (MRC) with stationary winding housing and its mathematical model are proposed based on the Bingham plastic model of MRF. Multi-objective design optimization for MRCs simultaneously considering power consumption, transmitting torque, and rotating mass is then studied based on the derived mathematical model and electromagnetic finite element analysis (FEA) of the MRC. Subsequently, an optimal configuration of the proposed MRC is manufactured and experimentally investigated.

Keywords: magnetorheological fluid (MRF), magnetorheological clutch, multi-objective optimization, speed control.

1. INTRODUCTION

Magnetorheological fluid (MRF) is a kind of smart fluid, which is composed of tiny magnetic particles (micro to nanometer scale) dispersed in a carrier (base) fluid. The MRF can be magnetized and exhibit fast (in few milliseconds), strong, and reversible changes in their rheological properties when a magnetic field is applied. Thanks to these special effects, the MRF holds great potentials in many applications requiring an electromechanical interface such as clutches, brakes, valves, dampers, and engine mount [1,2]. Therein, one of the most popular MRF-based devices attracting many researchers to investigate is the magnetorheological clutch (MRC).

There have been several studies on the development and implementation of different types of MRC during the two past decades. In the early stage, most of the researchers proposed the MRC configurations with rotating coils [3,4]. Which such configurations, the

main disadvantages are as follows: difficulties in manufacturing, unsteady and high friction due to brushes, "bottle-neck" problems of magnetic circuits. To overcome the above disadvantages, new configurations with stationary winding housing have been recently implemented. In this configuration, the coils of MRCs are wounded on a fixed housing, on which the input shaft (usually connected to the disc of the MRC) and the output shaft (usually connected to the housing of the MRC) are assembled [5, 6]. Recently, there have been several publications on the design and implementation of MRC in speed control of a rotary load shaft. Nguyen et al. [7] worked on the design and application of MRC in speed control of a DC motor. In this configuration, a magnetic coil was placed on a rotating housing of the clutch. The optimization of the MRC was conducted based on the FEA of the MRC magnetic circuit and the design objective is to minimize the mass while its transmitting torque is constrained to be greater than a certain value (10 Nm). First-order optimization method with steepest descent algorithm of ANSYS optimization tool was used to obtain the optimal solution. A PID controller was also implemented for tracking control of the output speed. A speed tracking error of 7% was obtained for a sinusoidal desired speed of 3Hz. In order to improve the accuracy of the controlled speed, more recently Nguyen et al. [8] proposed and implemented a new configuration of MRC with the coil placed separately out of the rotating housing of the clutch (in this paper, we denoted it as stationary housing MRC for short). Thanks to this proposed configuration, the coil is fixed and brushes are eliminated. Therefore, some disadvantages of conventional MRC such as magnetic flux "bottle-neck" problems, unsteady contact of the brushes, manufacturing difficulties, etc. can be handled. However, the design optimization of the MRC in this research only considers a single objective function (the moment of inertia of output part-the MRC housing) and uses the traditional gradient-based optimization technique as similar to the research [7]. For further investigations, Nguyen et al. [9] developed a speed control system of a rotary load shaft for the stationary housing MRC. In detail, the optimization of the MRC was conducted, in which the overall volume of the MRC system is minimized while the transmitted torque is subjected to be greater than 10 Nm. Experimental results on steady speed control of the rotary load shaft showed that an error of up to 3% was obtained for a load of 1 Nm while that in case of 5Nm load torque was up to 5%.

In previous study, only conventional gradient-based optimization algorithms dealing with single-objective design optimization were considered, which usually results in obtaining local optimum and poorly exploring valuable trade-offs among design objectives. In this research, a state-of-the-art multi-objective optimization approach is implemented and reveals some intrinsic relations of both design variables and design objectives into MRC structures.

2. MAGNETORHEOLOGICAL CLUTCH WITH STATIONARY HOUSING

Fig. 1(a) shows the conventional configuration of MRC [8], in which the coil is placed on the rotating housing connected to the output shaft of the MRC, while the stationary housing MRC proposed in the literature [9] is shown in Fig. 1(b).

(a) Conventional MRC   (b) Stationary-housing MRC

Fig. 1. Configurations of the conventional and the stationary-housing MRCs

The description of this configuration can be expressed as followings. A disc made of magnetic steel is fastened to the driving shaft made of non-magnetic steel. The disc is embedded inside the clutch housing. The housing is composed of two side housing parts made of magnetic material and a cylindrical (middle) housing one made of nonmagnetic material. A side housing part is connected to the driven shaft made of non-magnetic steel. The space between the disc and the housing is filled with MRF. Lip seals are used to prevent the leaking of MRF. The clutch housing is then placed in a stationary envelope, on which a magnetic coil is placed. To make sure that the clutch housing can freely rotate inside the envelope, there must be small air gaps between the housing and the envelope, and the housing and the coil. It is noteworthy that these should be as small as possible to not significantly weaken the strength of the applied magnetic field. As the coil is provided electric power, a magnetic field is generated as shown in Fig. 1(b) and the

MRF in the gaps becomes solid-like instantaneously. This results in a controllable torque transferred from the disc (the driving shaft) to the housing (the driven shaft). In Fig. 1, significant geometric parameters of both the conventional and the stationary-housing MRCs are also presented.

To determine the transmitting torque of MRC, we use the following assumptions in this study: MRF follows a Bingham plastic rheological model, and the velocity profile of the MRF is linearly distributed from the disc to the housing. With two above assumptions, the transmitting and the off-state torque of the MRC can be respectively determined by [9]

$$T = \frac{\pi \mu_e R_{do}^4}{d} \left[1 - \left(\frac{R_{di}}{R_{do}} \right)^4 \right] (\omega_i - \omega_o) + \frac{4\pi \tau_{ye}}{3} \left(R_{do}^3 - R_{di}^3 \right) + 2\pi R_{do}^2 t_d \left(\tau_{y0} + \mu \frac{(\omega_i - \omega_o) R_{do}}{d} \right) + T_{sf},$$
(1)

$$T_0 = \frac{\pi \mu_0 R_{do}^4}{d} \left[1 - \left(\frac{R_{di}}{R_{do}} \right)^4 \right] (\omega_i - \omega_o) + \frac{4\pi \tau_{y0}}{3} \left(R_{do}^3 - R_{di}^3 \right) + 2\pi R_{do}^2 t_d \left(\tau_{y0} + \mu \frac{(\omega_i - \omega_o) R_{do}}{d} \right) + T_{sf}.$$
(2)

In the above, R_{di} and R_{do} are the inner and outer radius of the disc, d is the MRF gap size, t_d is the thickness of the disc, ω_i and ω_o are respectively the angular velocity of the driving shaft and the driven shaft, τ_{ye} and μ_e are the average yield stress and post-yield viscosity of MRF in the end-face ducts, τ_{y0} and μ_0 are the zero-field yield stress and post-yield viscosity of the MRF, T_{sf} is the friction torque between the shaft of the clutch and the lip-seal friction torque T_{sf} can be estimated by [10]

$$T_{sf} = 0.65(2R_s)^2 \Omega^{1/3},$$
(3)

where T_{sf} is the friction torque of a lip seal in ounce-inches, Ω is the rotation speed of the brake shaft measured in rounds per minute, and R_s is the shaft diameter at the sealing measured in inches. It is noted that a field-dependent Bingham rheological model is implemented in this research, in which the induced yield stress τ_{ye} and the post-yield viscosity μ_e vary as a function of the exerted magnetic flux density across the ducts of MRF and they are estimated by the following equations [11]

$$\tau_{ye} = \tau_{y\infty} + (\tau_{y0} - \tau_{y\infty})(2e^{-B\alpha_{SY}} - e^{-2B\alpha_{SY}}),$$
(4)

$$\mu_e = \mu_\infty + (\mu_0 - \mu_\infty)(2e^{-B\alpha_{SY}} - e^{-2B\alpha_{SY}}),$$
(5)

where $\tau_{y\infty}$ and μ_∞ are the yield-stress and post-yield viscosity of MRF at the state of magnetic saturation, α_{SY} is the saturation moment index, B is the applied magnetic density across the MRF duct. To calculate the values of B, the FEA approach is implemented via the commercial ANSYS software in this study. Fig. 2 shows finite element models of two considered MRCs using 2D-axisymmetric couple element PLANE 13 for magnetic analysis. It is noted that the meshing sizes of the models are controlled by the number of elements in each line.

(a) Conventional MRC

(b) Stationary-housing MRC
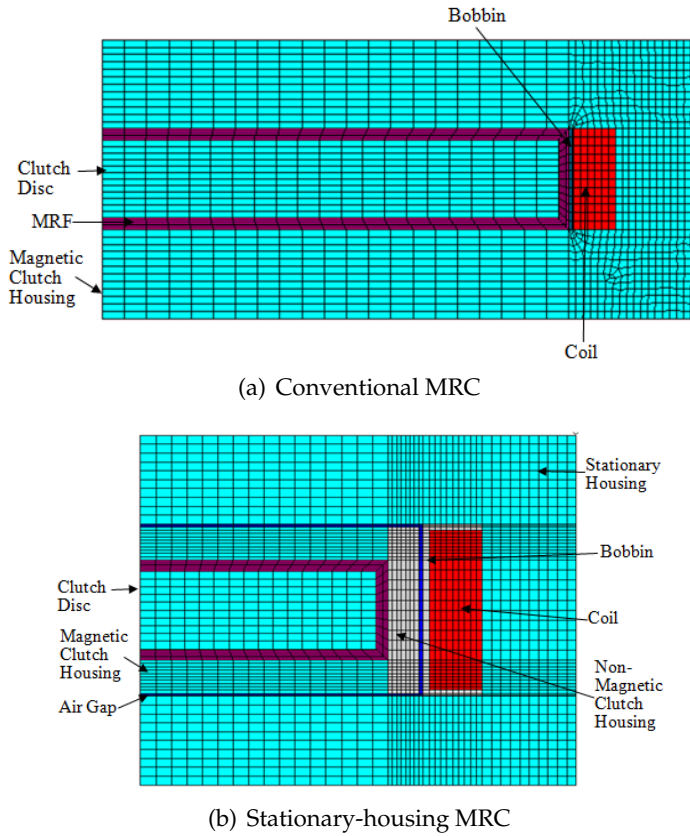
Fig. 2. Finite element models to analyze magnetic circuit of two considered MRCs

3. MULTI-OBJECTIVE DESIGN OPTIMIZATION OF MAGNETORHEOLOGICAL CLUTCH

3.1. Problem statement

In this study, a multi-objective optimization problem is conducted in view of simultaneously optimizing different design objectives of MRCs. Two design objectives of MRCs are taken into account include total mass and transmitting torque. The multi-objective design problem is then expressed as follows

Minimize $\begin{cases} f(1) = m_c \\ f(2) = -T \end{cases}$

Subject to $x_i^L \leq x_i \leq x_i^U, i = 1, \ldots, n$

Therein, the total weights of MRCs are generally expressed by

$$m_c = V_d \rho_d + V_h \rho_h + V_s \rho_s + V_{MR} \rho_{MR} + V_{bob} \rho_{bob} + V_c \rho_c, \tag{6}$$

where V_d, V_h, V_s, V_{MR}, V_{bob}, and V_c are respectively the geometric volume of the disc, the housing, the shaft, the MRF, the bobbin and the coil of the clutch; ρ_d, ρ_h, ρ_s, ρ_{MR}, ρ_{bob} and ρ_c are correspondingly density of the discs, the housing, the shaft, the MRF, the bobbin and the coil material; x_i^L, x_i^U are the lower and upper bounds geometric dimensions of each design variable x_i; and n is the number of design variables. The transmitting torque T is evaluated by Eq. (1).

Power consumption P is calculated as follows

$$P = I^2 \Omega_c, \tag{7}$$

where I is the current magnitude applied to the coil and Ω_c is the resistance of the coil which can be estimated by

3.2. Optimization method
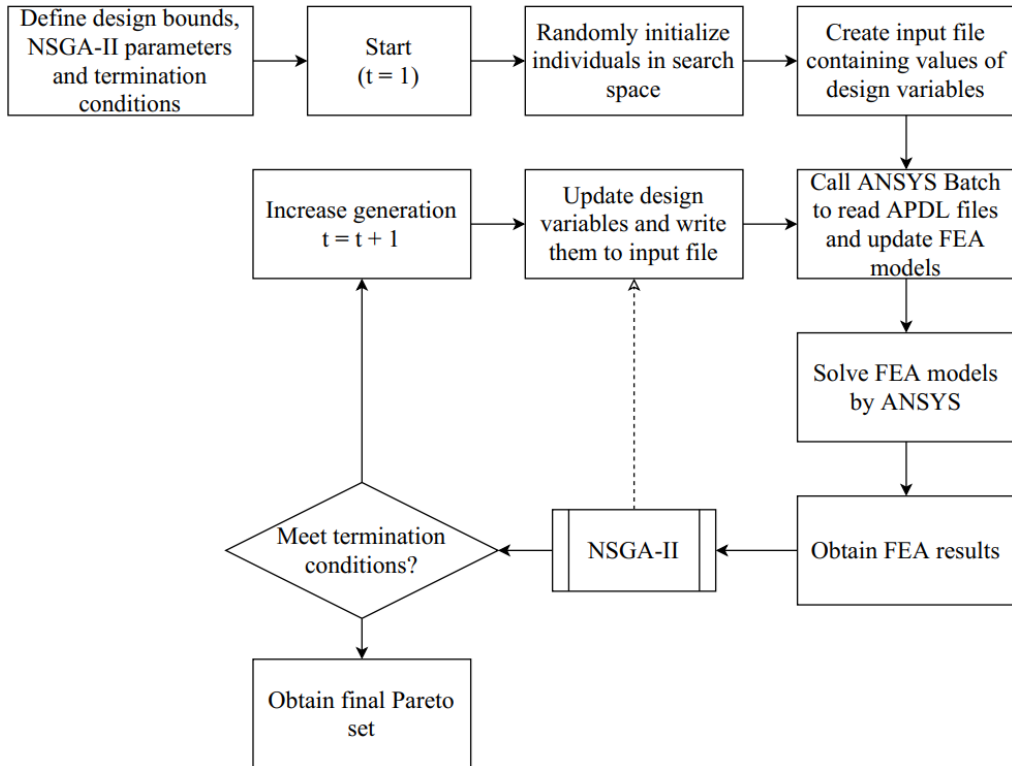
Fig. 3. Flowchart of integrated optimization method using NSGA-II

In this study, a well-known metaheuristic method called Non-dominated Sorting Genetic Algorithm (NSGA-II) [12, 13] is applied for the multi-objective design optimization of. It is noted that NSGA-II was successfully applied to investigate various optimization problems in the literature [14, 15]. The flowchart of the integrated optimization method

using NSGA-II is shown in Fig. 3. Herein, NSGA-II is combined with ANSYS in a loop procedure to solve the multi-objective design optimization of MRCs.

Firstly, a population containing design data is generated in Matlab via NSGA-II codes. These data are then written into input files for creating corresponding FEA models in ANSYS. To analyze the magnetic behaviors of the MRCs, a 2D-axisymmetric couple element PLANE13 is used to solve the magnetic circuits to obtain the magnetic density across the MRF gaps. These values are applied to estimate MRF rheological parameters including yield stress and post-yield viscosity via Eqs. (4) and (5). Matlab subsequently reads and uses these parameters to evaluate the transmitting torque according to Eqs. (1) and (3). The value of objective function is subsequently analyzed by NSGA-II to gain the Pareto set. The termination conditions are also checked at this step to determine if the final Pareto set is obtained or not. In case the termination conditions are not satisfied, NSGA-II updates the design variables and the optimization loop will repeat until the termination conditions are fully met.

3.3. Numerical results

Both the conventional and the proposed MRCs are investigated in this section. It is noted that the C45 Steel is used for magnetic parts of MRCs and commercial MRF132-DG is used to fill the gaps between disc and housing which are fixed at 0.8 mm. The rheological parameters of MRF132-DG used for calculating the induced yield stress and yield viscosity in Eqs. (4) and (5) are given as follows: τ_{y0} = 15 Pa, μ_0 = 0.1 Pa.s, $\tau_{y\infty}$ = 40,000 Pa, μ_∞ = 3.8 Pa.s, $\alpha_{S\mu}$ = $4.5T^{-1}$, $\alpha_{S\tau y}$ = $2.9T^{-1}$. The diameter of copper wires is 0.51 mm (24 gauge wire) and its maximum working current intensity is 2.5A. As mentioned in Section 2, the air gap between stationary and rotation housings for the case of stationary-housing MRC must be as small as possible to maximize the strength of the magnetic field considering manufacturing and maintenance issues. Therefore, a small air gap of 0.3 mm is set between the housing and the side envelopes, and a gap of 1.0 mm is set between the housing and the coil. The bobbin thickness and the shaft radius in both the convention and the proposed MRCs are respectively fixed at 0.5 mm and 6 mm. It is noted that for input magnetic property of the C45 Steel and MRF132-DG, B-H curve is implemented. In addition, a relative permeability of 1.0 is assumed for non magnetic materials such as copper wire and bobbin. A current density is applied to the area of the coil and a parallel flux lines are set at the boundary of the MRCs.

Figs. 4(a) and 4(b) respectively shows Pareto fronts of the transmitting torque with respect to both the total and rotating mass of two considered MRCs. In these figures, it is noted that in "Case 1" the power consumption is not taken into account as an objective while in "Case 2" it is taken into account as an objective function. It is easily realized that the transmitting torque and the mass of MRCs have trade-off benefits. The higher the transmitting torque is, the greater the MRC sizes increase. Fig. 4(a) presents that the total mass of the stationary-housing MRC is much higher than those of the conventional one considering the same induced transmitting torque, which results in the increment
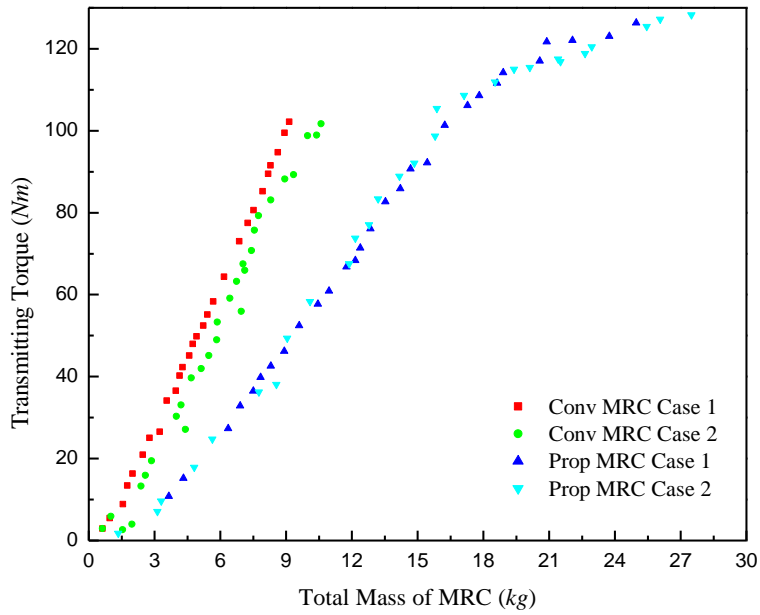
(a) Transmitting torque vs. total mass
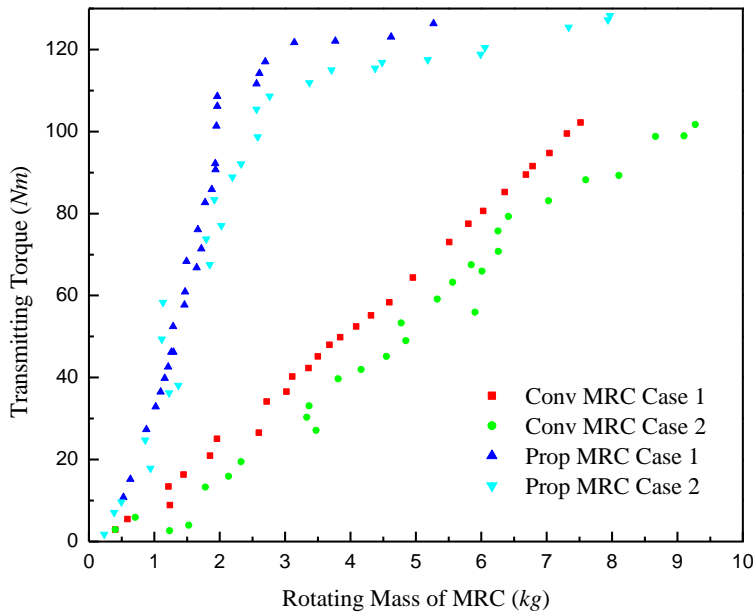
(b) Transmitting torque vs. rotating mass

Fig. 4. Pareto set of the mass and transmitting torque of the MRCs

of material used to manufacture the proposed clutch. However, the rotating mass obtained from the stationary-housing MRC in Fig. 4(b) is much lighter than those of the remaining one, which reveals some potential advantages for control output speed of the proposed MRC because the smaller weight of its rotating parts can significantly reduce inertia effect.

4. OPTIMAL DESIGN AND EXPERIMENTAL RESULTS OF MRC PROTOTYPE

In this section, design optimization for two considered MRCs is conducted to determine their optimal sizes for prototype manufacturing. Design optimization aims to optimize the structural configuration of the clutch so that its transmitting torque must be greater than a required one while its mass is minimized. It is noted that the optimal results can be roughly obtained from multi-objective optimization results. However, in order to obtain a better exact optimal solution, the multi-objective optimal solution should be refined. In this research, optimal results obtained from the multi-objective optimization are used at initial values of design variables, and the first-order optimization method integrated into the ANSYS optimization tool is used to find the refined optimal results.

Table 1. Parameters of the optimized MRCs

Types of MRC	Design Variable (mm)	Characteristic
Conventional MRC	Disc: $R_i = 18.755$, $R_d = 52.81$ Housing: $R = 62.46$, $L = 16.78$ Coil: $R_w = 58.046$, $h_c = 4.935$ MRF: $d = 0.8$	$T = 9.9816$ Nm $m_c = 1.6044$ kg $P = 22.605$ W
Stationary-housing MRC	Disc: $R_i = 19.996$, $R_d = 53.299$ Outer-housing: $R = 69.181$, $L = 20.538$ Coil: $R_w = 54.799$, $h_c = 7.633$ MRF: $d = 0.8$	$T = 9.9003$ Nm $m_c = 2.4087$ kg $P = 45.223$ W

Table 1 summarizes the important dimensions of the optimized MRCs and their characteristics including total mass, transmitting torque, and power consumption. Fig. 5 presents the density distribution of the magnetic field inside the MRCs. It is seen that the magnetic fields in Fig. 5 are highly dense in the regions around the coil and gradually spare along the radius of MRCs which results in "bottle-neck" problem. This "bottle-neck" problem reduces the magnetic flux across the MRF gaps and then decreases the performances of these MRCs. It is clearly observed that the "bottle-neck" problem of the conventional MRC is more severe than that of the stationary housing one. From the optimal results, prototypes of the MRCs are manufactured as displayed in Fig. 6.

(a) Conventional MRC

(b) Stationary-housing MRC
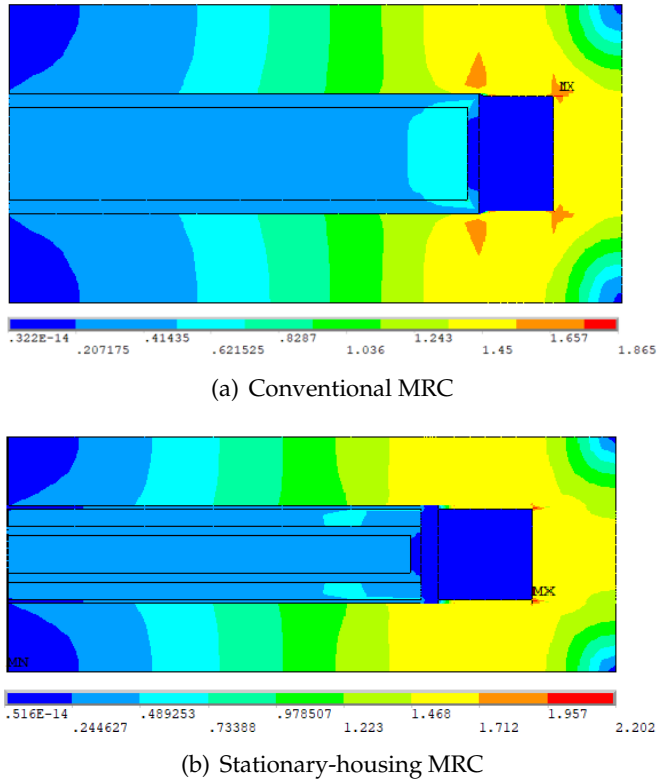
Fig. 5. Magnetic density distribution of the MRCs at the optimum, $T = 10$ Nm

(a) Conventional MRC

(b) Stationary-housing MRC

Fig. 6. Prototypes of the optimized MRCs

Table 2. Main components of the MRC test rig

Parts	Characteristics
Torque Sensor	TS20
Amplifier	LCV-U10
MRC	10 Nm
AC Servo	MSMD022S1T
Programmable Power Supply	PPW-8011
Data Acquisition	NI-Myrio 1900
Gearbox	15:1
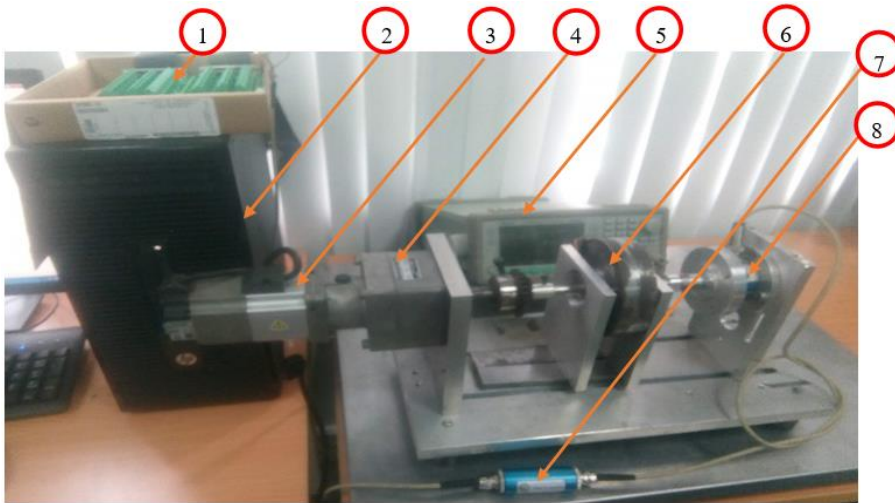
Fig. 7. Torque measurement of MRC in bench test: (1) DAQ, (2) computer, (3) AC Servo,
(4) gearbox, (5) programmable supply, (6) MRC prototype, (7) amplifier, (8) Torque transducer

Table 2 presents the necessary components for building the experimental test for speed control of MRCs. The experimental setup for the torque measurement of MRCs is shown in Fig. 7. In this figure, an AC servo motor is used to drive the driving shaft of the MRC via a gear-box at a constant angular speed of 120 rpm. The housing of the MRC is fixed to make the clutch work as a brake. A torque sensor is applied to measure the torque generated by the clutch. After that, the output signal from the torque sensor is transferred to a computer via a DAQ system for evaluation. To conduct the experimental test, the computer sends step current signals to a programmable supplier. The output current of the supplier with its current step of 0.5A is applied to the coil of MRC and the corresponding values of average output torque is evaluated on the computer. The relation between the measured torque and the input current is shown in Fig. 8. It is observed that at the applied current of 2.5A, the measured torque is almost reached to 10 Nm as simulated. A least squared curve fitting method is used to express the generated torque

of MRCs as a function of the input currents, and they are presented as follows

$$T_c = -0.049 + 3.076I + 2.283I^2 - 0.766I^3, \tag{8}$$

$$T_p = -0.06 + 3.161I + 2.319I^2 - 0.8I^3, \tag{9}$$

where T_c and T_p are respectively the torque generated by the conventional and the stationary-housing MRC, and I is the magnitude of the step current applied to the coil.
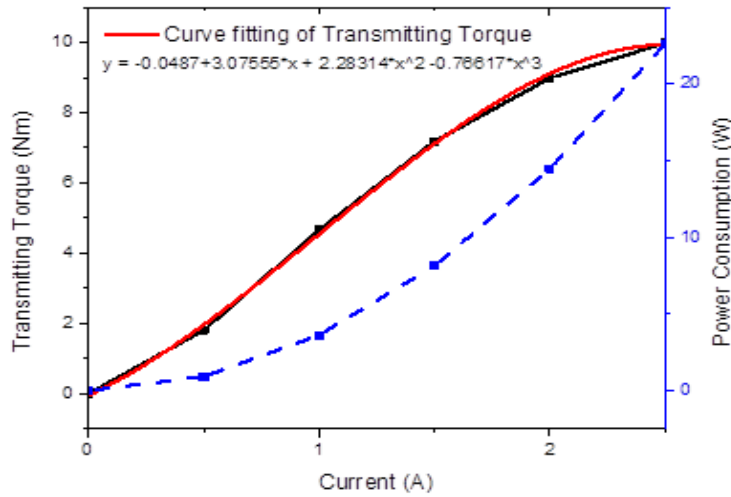
(a) Conventional MRC
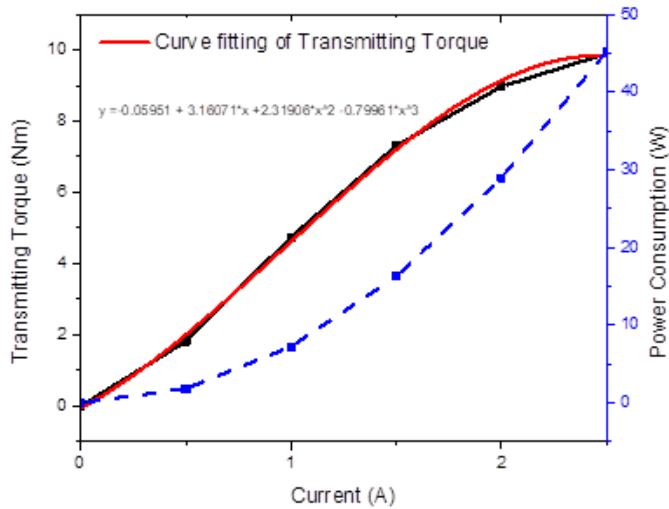
(b) Stationary-housing MRC

Fig. 8. Transmitting torque as a function of current

5. CONCLUSIONS

In this study, multi-objective optimal design of a new type of MR clutches is performed and experimentally evaluated. Firstly, a new configuration of MRC with coils placed on stationary housing was proposed to eliminate existed shortcomings of the conventional one. A mathematical model of the proposed MRC was derived based on the Bingham plastic model of MRF. Multi-objective design optimization of the two MRCs was subsequently conducted considering simultaneously mass and transmitted torque. The multi-objective optimal results clearly showed the trade-off between the transmitting torque and the rotating mass of all MRCs. It was also shown that those of the stationary-housing clutch were generally better than those of the conventional one when comparing in pairs. For MRC prototypes, single-objective design optimization (minimization of MRC mass) was implemented to determine the best structures of MRCs with initial values of design variables obtained from the multi-objective optimization in case the transmitting torque is 10 Nm. It was shown that a good agreement between the experimental results and simulated one was archived. It is finally noted that although structures of proposed MRC is more complicated than that of conventional MRC, it can solve the inherent problems of the conventional one such as unsteady and high friction due to brushes, "bottle-neck" magnetic problem.

DECLARATION OF COMPETING INTEREST

The authors declare that they have no known competing financial interests or personal relationships that could have appeared to influence the work reported in this paper.

ACKNOWLEDGMENT

REFERENCES

[1] J. Wang and G. Meng. Magnetorheological fluid devices: Principles, characteristics and applications in mechanical engineering. *Proceedings of the Institution of Mechanical Engineers, Part L: Journal of Materials: Design and Applications*, **215**, (2001), pp. 165–174. https://doi.org/10.1243/1464420011545012.

[2] A. Muhammad, X. liang Yao, and Z. chao Deng. Review of magnetorheological (MR) fluids and its applications in vibration control. *Journal of Marine Science and Application*, **5**, (2006), pp. 17–29. https://doi.org/10.1007/s11804-006-0010-2.

[3] U. Lee, D. Kim, N. Hur, and D. Jeon. Design analysis and experimental evaluation of an MR fluid clutch. *Journal of Intelligent Material Systems and Structures*, **10**, (1999), pp. 701–707. https://doi.org/10.1106/ex6x-y4qq-xq5l-8jjv.

[4] T. Kikuchi, K. Ikeda, K. Otsuki, T. Kakehashi, and J. Furusho. Compact MR fluid clutch device for human-friendly actuator. *Journal of Physics: Conference Series*, **149**, (2009). https://doi.org/10.1088/1742-6596/149/1/012059.

[5] D. Wang and Y. Hou. Design and experimental evaluation of a multidisk magnetorheological fluid actuator. *Journal of Intelligent Material Systems and Structures*, **24**, (2012), pp. 640–650. https://doi.org/10.1177/1045389x12470305.

[6] K. H. Latha, P. U. Sri, and N. Seetharamaiah. Design and manufacturing aspects of magnetorheological fluid (MRF) clutch. *Materials Today: Proceedings*, **4**, (2), (2017), pp. 1525–1534. https://doi.org/10.1016/j.matpr.2017.01.175.

[7] Q. H. Nguyen and S.-B. Choi. A new method for speed control of a DC motor using magnetorheological clutch. In W.-H. Liao, editor, *SPIE Proceedings*, SPIE, (2014). https://doi.org/10.1117/12.2044558.

[8] Q. H. Nguyen and S.-B. Choi. A new method for speed control of a DC motor using magnetorheological clutch. In *Active and Passive Smart Structures and Integrated Systems 2014*, SPIE, SPIE, Vol. 9057, (2014), pp. 882–888.

[9] T. D. Truong, V. Q. Nguyen, B. T. Diep, D. H. Q. Le, D. T. Le, and Q. H. Nguyen. Speed control of rotary shaft at different loading torque using MR clutch. In A. Erturk, editor, *Active and Passive Smart Structures and Integrated Systems XIII*, SPIE, (2019). https://doi.org/10.1117/12.2515309.

[10] EPS Division. *Rotary seal design guide*. Parker Hannifin Corporation, Catalog EPS 5350, (2006).

[11] Q. H. Nguyen, N. D. Nguyen, and S. B. Choi. Design and evaluation of a novel magnetorheological brake with coils placed on the side housings. *Smart Materials and Structures*, **24**, (2015). https://doi.org/10.1088/0964-1726/24/4/047001.

[12] C. A. C. Coello. Evolutionary multi-objective optimization: a historical view of the field. *IEEE Computational Intelligence Magazine*, **1**, (2006), pp. 28–36. https://doi.org/10.1109/mci.2006.1597059.

[13] K. Deb, A. Pratap, S. Agarwal, and T. Meyarivan. A fast and elitist multiobjective genetic algorithm: NSGA-II. *IEEE Transactions on Evolutionary Computation*, **6**, (2002), pp. 182–197. https://doi.org/10.1109/4235.996017.

[14] V. Ho-Huu, D. Duong-Gia, T. Vo-Duy, T. Le-Duc, and T. Nguyen-Thoi. An efficient combination of multi-objective evolutionary optimization and reliability analysis for reliability-based design optimization of truss structures. *Expert Systems with Applications*, **102**, (2018), pp. 262–272. https://doi.org/10.1016/j.eswa.2018.02.040.

[15] T. Le-Duc, V. Ho-Huu, and H. Nguyen-Quoc. Multi-objective optimal design of magnetorheological brakes for motorcycling application considering thermal effect in working process. *Smart Materials and Structures*, **27**, (2018). https://doi.org/10.1088/1361-665x/aacb40.